Astron. Astrophys. 345, 999–1005 (1999)

ASTRONOMY AND ASTROPHYSICS

Detection of the O VI 103.2 nm line polarization by the SUMER spectrometer on the SOHO spacecraft

N.-E. Raouafi[1,2], **P. Lemaire**[1], **and S. Sahal-Bréchot**[2]

[1] Institut d'Astrophysique Spatiale, Unité mixte CNRS – Université Paris XI, F-91405 Orsay, France
[2] Département 'Atomes et molécules en Astrophysique', Unité Associée au CNRS n°812, Observatoire de Paris-Meudon, 5 place Jules Janssen, F-92195 Meudon Cedex, France
(Nour-Eddine.Raouafi@medoc-ias.u-psud.fr; raouafi@obspm.fr; lemaire@ias.fr; Sylvie.Sahal-Brechot@obspm.fr)

Received 2 December 1998 / Accepted 4 February 1999

Abstract. The first detection of the O VI 103.2 nm line polarization has been performed in the corona by SUMER (Solar Ultraviolet Measurements of Emitted Radiation) on the SOHO (Solar Heliospheric Observatory). The polarization properties of the spectrometer was used to analyze the solar radiation in a coronal hole at about 270 arcsec above the south solar limb, during the SOHO spacecraft rotation of March 19, 1996. Taking advantage of the different behavior of the lines in the O VI doublet and of the nearby chromospheric lines we have been able to extract the weak signal modulation introduced by polarization from solar variations and telescope scattered light. The $\approx$ 4% modulation rate (related to the linear polarization of the O VI 103.2 nm line) derived is an important clue to infer the properties of the local magnetic field strength and the velocity field in the coronal hole.

Key words: polarization – Sun: corona – Sun: UV radiation

1. Introduction

The knowledge of vectorial quantities, such as magnetic and velocity fields which lie in the solar corona and the region of the solar wind acceleration, are of capital importance to understand physical processes such as coronal heating and acceleration of the solar wind. Determination of vectorial quantities is much more difficult than the determination of scalar ones. Scalar quantities, such as temperatures and densities, are obtained through spectroscopic diagnostic methods, based on analysis of profiles and intensities of adequately selected lines. Vectorial quantities can be obtained through spectropolarimetric analysis, *i.e.* interpretation of the Stokes parameters. The determination of vectorial quantities (such as magnetic and matter velocity fields) from the measurement of polarization parameters of adequate lines is very important for MHD modelling.

Some permitted emission lines (such as Li-like ion lines: O VI, N V, C IV,...) seen above the solar limb high in the corona should be affected by the coronal mass flow through the so-called Doppler dimming effect (Gabriel, 1971; Beckers & Chipman, 1974; Kohl & Withbroe, 1982; Withbroe et al., (1982a, 1982b)). These lines are partially formed and linearly polarized through a resonance scattering mechanism: the coronal moving atoms and ions absorb the anisotropic radiation emitted by the same atoms and ions of the underlying solar transition region. Due to the Doppler effect, the absorption takes place somewhere in the wing of the incident line radiation, leading to a decrease of the coronal scattered intensity and an increase of the line width by absorption and reemission at some distance of the zero velocity line center. Moreover, the linear polarization parameters of the scattered line are modified by the Doppler effect (Sahal-Bréchot et al., 1992, 1998). In addition these linear polarization parameters are sensitive to the local magnetic field vector through the Hanle effect (Sahal-Bréchot, 1981; Sahal-Bréchot et al., 1986). Bommier et al. (1994) and previous related papers (Sahal-Bréchot et al., 1977; Bommier & Sahal-Bréchot, 1978; Bommier et al., 1986; and so on) have successfully demonstrated the power of the Hanle effect method for measuring the magnetic field vector of solar prominences. Consequently it can be inferred that the measurement of polarization parameters of well-chosen coronal lines will permit one to get complete information about strengths and direction of both the velocity field and magnetic field vectors, through interpretation of Doppler-dimming and Hanle effects.

Li-like ion lines (O VI, N V, C IV,...), which are presumed to be observed high in the corona due to their broad abundance curves (Sahal-Brechot et al., 1986), have small natural widths owing to the short lifetimes of the upper levels of the corresponding atomic transitions and then give a magnetic field strength corresponding to their sensitivity to the Hanle effect who ranges from a few Gauss to more than 300 Gauss. Such interval contains the expected magnitude of the magnetic field strength in the solar polar coronal holes. Li-like ion lines are very intense lines of the chromosphere-corona transition region (the O VI 103.2 nm line is presumed to be one of the most intense lines after H I *Ly* α). The observed emission of O VI ion by Vial et al. (1980) at $30''$ above the limb (as well as Reeves and Parkinson, 1970) has shown that the O VI emission extends out into the corona to a few arcmin above the limb (Vial et al., 1980). Recent measure-

Send offprint requests to: N.-E. Raouafi
(raouafi@medoc-ias.u-psud.fr; raouafi@obspm.fr)

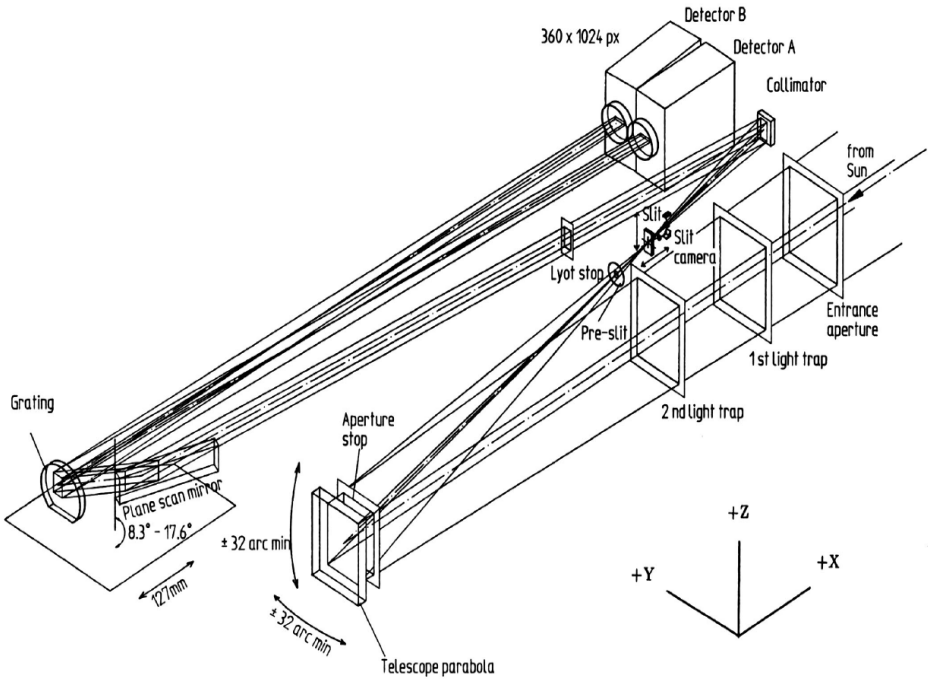

Fig. 1. The optical layout of the SUMER instrument showing the different optical components conducting the light from the entrance aperture to the detectors. SUMER sensitivity to the polarization of the incident light arises from the wavelength scan mirror and the grating. The wavelength scan mirror receive light under a large incidence angle, which ranges from 73.3° to 81.6° (with respect to the mirror normal). That lets it to act as a linear polarizer. Similarly, the incidence angles of light reflected by the plane mirror and incoming on the grating vary from 16.7° and 35.0° and it acts as a second linear polarizer (from Wilhelm et al., 1995).

ments from UVCS/SOHO show the O VI emission several solar radii above the limb, with a line ratio and line widths sensitive to Doppler dimming and anisotropic velocity distributions (Kohl et al., 1998; Li et al., 1998).

The upper level $2p\ ^2P^0_{3/2}$ of this resonance line is populated from the ground state both by electronic collisions and by absorption of the same line emitted by the underlying transition region zone. Electronic collisions are isotropic and cannot create polarization. The incident transition zone radiation is unpolarized but anisotropic, thus the reemitted coronal line can be partially linearly polarized (resonance fluorescence scattering), as in the case of forbidden lines of the corona (Sahal-Bréchot, 1974, paper I and II; Sahal-Bréchot, 1977). However, contrary to the case of forbidden lines, electron and proton collisions cannot depolarize efficiently the upper level of the O VI resonance line, because its lifetime is very short: in other words, the photon is emitted before the alignment of the excited level is destroyed by collisions redistributing the populations of the substates.

The SUMER (Solar Ultraviolet Measurements of Emitted Radiation) spectrometer on SOHO (Solar Heliospheric Observatory) spacecraft is sensitive to the state of polarization of the incident radiation. The wavelength range of the SUMER spectrometer contains the O VI 103.2 nm and 103.7 nm lines. The first one (a $\frac{1}{2} \longrightarrow \frac{3}{2}$ transition) can be partially and linearly polarized and one of the most intense coronal lines after H I *Ly* α line. The second one (a $\frac{1}{2} \longrightarrow \frac{1}{2}$ transition) is not polarized. SUMER spectrometer can be used as an analyser for the state of polarization of the O VI 103.2 nm line. To do that we have to take advantage of the rotation of the whole spacecraft. The rotation of the analyser of polarization is performed by a rotation of the whole instrument along the pointing axis in keeping the same area in the corona inside the spectrometer slit.

The present paper aims are to show the use of the SUMER spectrometer on SOHO to study the polarization of the O VI 103.2 nm line. In Sect. 2, we recall the main properties of SUMER as a spectrometer and we detail the properties of SUMER as an analyser of linear polarization. In Sect. 3, a brief presentation of the observations is made and we give the procedures used to reduce these observations. The correction of the scattered light is presented in detail in Sect. 4. The building of monochromatic images is developped in Sect. 5. The results are discussed in Sect. 6.

2. Polarization sensitivity of the SUMER instrument on SOHO

SUMER is one of the twelve instruments on the ESA/NASA SOHO spacecraft which was launched in December 1995. The SUMER optical design is shown in Fig. 1. It is constituted of a normal incidence telescope, a Wadsworth configuration concave grating spectrometer and a microchannel plate array detector. Its spectral bandpass ranges from 500 to 1610 Å. In this wavelength range it is possible to observe emission lines of atoms and ions of the chromosphere, chromosphere-corona transition region, and corona. Therefore it is possible to diagnose the solar atmosphere by measuring profiles and intensities of these UV lines. The line profiles and intensities permit the study of local properties of the external solar layers (densities, temperatures, matter motion,...) (Wilhelm et al., 1997; Lemaire et al., 1997; Hassler et al., 1997; Doschek et al., 1997; Judge et al., 1997, Brekke et al., 1997). SUMER can observe with high spatio-temporal and spectral resolution. It has an angular resolution of about 1 arcsec (equivalent to 700 km in spatial extend), a temporal resolution down to 1 sec, and spectral resolving power $\lambda/\Delta\lambda = 17700 - 38300$ (Wilhelm et al., 1995).

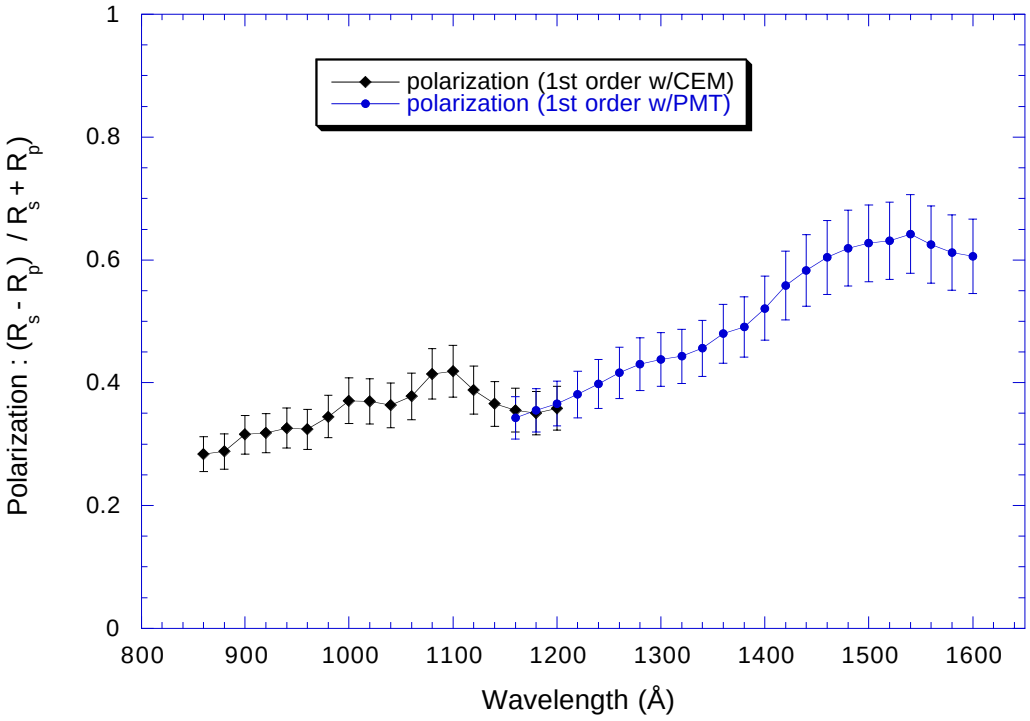

Fig. 2. Summary of the measured polarization sensitivity (modulation) of the SUMER instrument from 800 to 1600 Å. R_s and R_p are the intensities of the reflected radiation (by the wavelength scan mirror and the holographic grating) respectively parallel and perpendicular to the direction of polarization of the incident beam. Error bars represent roughly one sigma (68%) confidence level in the measured values (taken from Hassler et al., 1997, Fig. 6.)

The SUMER instrument is sensitive to the state of linear polarization of the incident radiation via two of its optical components: the wavelength scan mirror and the holographic grating. The scan mirror collects the parallel beam issued from the collimator under a large angle of incidence and plays the role of a linear polarizer. The light reflected by the scan mirror is sent to the holographic grating. This angle of incidence on the scan mirror varies, with respect to the normal to the scan mirror, from $73.3°$ to $81.6°$. The incidence angle on the grating ranges between $16.7°$ and $35.0°$ and the grating acts as a second polarizer beyond the scan mirror. The polarization sensitivity of the microchannel plate detector is very small compared to that of the wavelength scan mirror and the grating. We assume that the polarization modulation is due only to the two latter optical components (Hassler et al., 1997).

The SUMER spectrometer's performances as an analyser of linear polarization of an incident radiation were measured with the engineering model optics in the Institut d'Astrophysique Spatiale (IAS) in Orsay-France. The spectrometer model was put in a vacuum chamber fed by synchrotron radiation. The light issued from the synchrotron ring is nearly 100% linearly polarized in the orbital plane of the accelerated positron, in the SUPER Anneau de Collisions d'Orsay (SUPERACO) positron storage ring. The measured polarization sensitivity of the SUMER instrument is shown in Fig. 2 (taken from Hassler et al., 1997, Fig. 6). The SUMER's sensitivity to the linear polarization varies with the wavelength from roughly 30% to more than 60%. This is verified for the two spectral orders of the grating. The variation with wavelength is important in the first order as seen in Fig. 2.

3. Observations

The results discussed in this paper were derived from observations taken by the SUMER spectrometer on the SOHO spacecraft in March 19, 1996. The series of observations began in March 19, 1996 at 14:01 UT and finished in March 20, 1996 at 04:37 UT. It consists in observing a coronal region in the solar south polar hole at about 270 arcsec above the solar limb in the wavelength range 102.1 - 104.1 nm, which contains H I *Ly* β line at 102.5 nm, the O VI 103.2/103.7 nm lines, C II 103.6 nm, and several others weak lines. These observations were done by performing raster sequences to build monochromatic images of the observed region, using a of 4 * 300 arcsec^2 slit; the data collected on half of the detector A were transmitted to the ground station. A typical SUMER image of the detector taken from the roll dataset we are analysing is shown in Fig. 3. The strong lines of H I *Ly* β, O VI are prominent. The weaker lines of C II and O I will be used for the wavelength calibration. The two chromospheric lines of C II will be also used to correct the instrumental scattered light due to the SUMER's telescope.

Taking advantage of the SOHO roll maneuver performed in March 19, 1996, we were able to carry out rasters from the same area of the south polar hole under different angular positions of the slit in reference to the projected north-south solar axis (hereafter angle of observation): $0°, 30°, 60°, 90°, 135°, 180°$. Each raster contains 15 slit positions with a step size of 4 arcsec, except the $0°$ rasters which contain 31 slit positions with the same step size. Two rasters were taken at $0°, 90°$, and $180°$. The exposure time for a spatial position of the slit is 120 sec.

To correct for the nonuniform sensitivity of the detector, it was necessary to flat-field the data. A flat-field detector image,

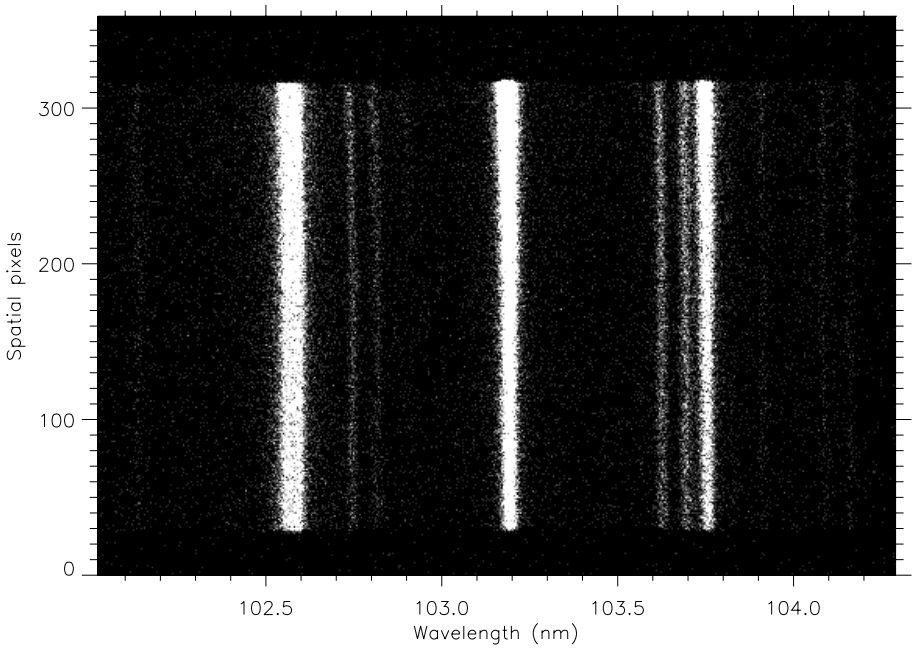

Fig. 3. A typical image of the detector at a slit position for a raster at 0°. We recognize clearly the strong lines of Ly β at 102.57 nm, O VI at 103.19 nm and 103.76 nm. The chromospheric lines of C II at 103.6 nm which are pure scattered light serve for the scattered light correction. We remark also the existence of other weak lines of O I. The variation of the line intensities along the slit is due to the fact that one extremity of the slit is closer to the solar limb than the other.

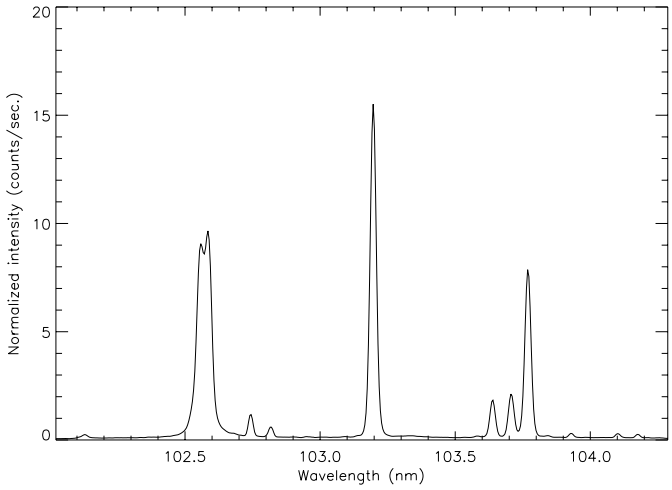

Fig. 4. A spectrum of the SUMER's scattered light obtained by integration along the spatial pixels (along the slit) from an image taken high in the corona (at more than one solar radius from the solar limb). This spectrum gives us the line profiles of the SUMER's scattered light in addition to the positions of the different lines. We can also extract the rate of scattered light in a given line via the ratio of the intensity of this line to that of the C II line presumed to be formed entirely by scattered light.

taken in february 28, 1996 at 14:20 UT with a 1 * 300 arcsec^2 slit for a long exposure time (more than 3 hours) at the wavelength 880 Å and with the grating kept defocused, was used to do this correction. This image was chosen to be the nearest in time of our observations, this is done to minimize the errors due to time variation effects of the detector.

In addition to its nonuniform sensitivity, the detector presents a geometrical distortion. This geometrical distortion gives a mispresented image of the slit, which is bended (curved) and inclined with respect to the columns of the detector. The deformation of the image of the slit (curvature and inclination in relation to the columns of the detector) may slightly depend on the wavelength. The image of the slit given by the detector appears shorter at the center than at the edges of the detector. To correct this geometric distortion of the images given by the detector, we have used the program developed by T. Moran (1996). This program is based on the comparison of the image of a regular rectangular grid given by the detectors of SUMER (taken before the launch of SOHO) and the regular grid.

4. Correction of the scattered light

After the flat-field correction and the correction of the distorted images by using Moran's procedure described above, all the images must be corrected from the light scattered by the instrument and specifically by the telescope mirror. This correction is very important above the limb: it is the substraction of a straylight signal and a wrong correction can introduce a noise which may be more important than the expected variation of the intensity of O VI 103.2 nm with the angle of observation. To do that we should know the profile and the location of the scattered light lines of SUMER, in addition to the rate of scattered light that must be subtracted for a given line. For this an image of pure scattered light has been taken far from the solar limb image (about 1000 arcsec above the solar limb) in July 20, 1996 at 4:12 UT in the wavelength range 102.1 - 104.1 nm with a 1 * 300 arcsec^2 slit and a long exposure time (more than 2 hours). By a convolution one can build an equivalent image taken by a 4 * 300 arcsec^2 slit. The flat-field correction of the scattered image is performed by a flat-field image taken in July 25, 1996 at 3:05 UT, and as before the geometric distortion is done by using Moran's procedure.

At such a height in the corona (one solar radius) the observed emission is only the light scattered by the telescope mirror. As

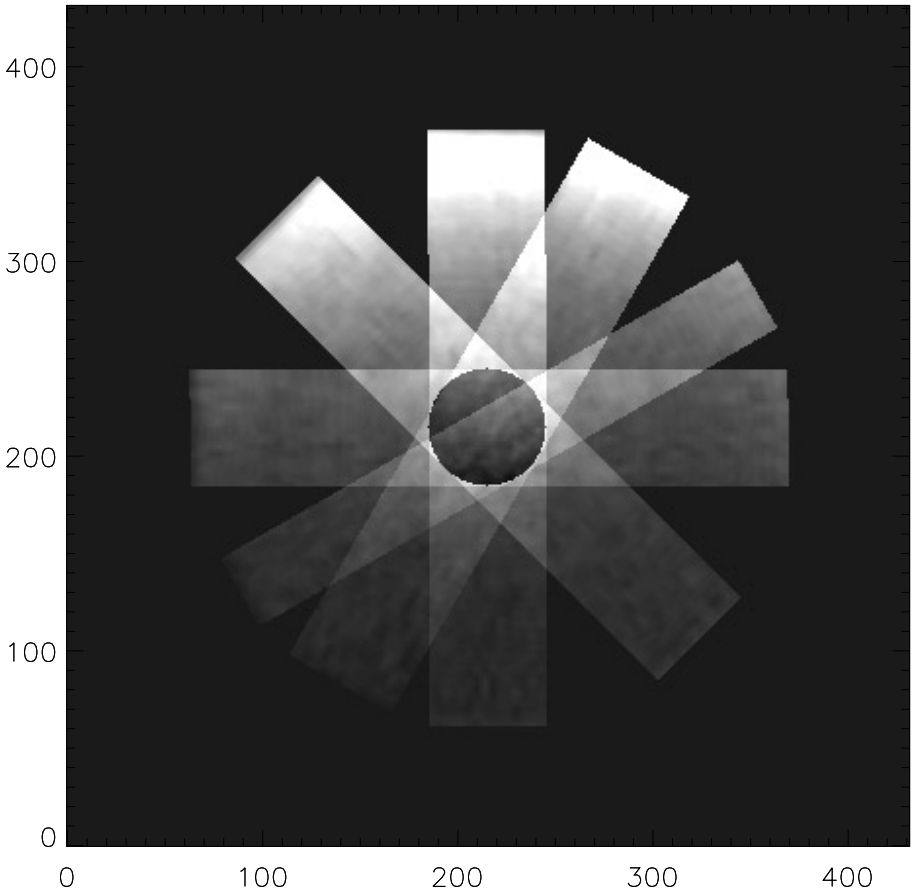

Fig. 5. The superposition of the monochromatic images (in this figure: $\lambda = 103.2$ nm) corresponding to the different rasters (with respect to their angles of observation), performed during the rotation of the SOHO spacecraft. The common part represents the same area in the corona, analyzed under different angles. The variation of the integrated intensity of the O VI 103.2 nm line in this part with the angle gives us information about its polarization. Some rasters are narrower than the others, this is due to elimination of some slit positions in these rasters which are taken before the stabilization of SOHO at the corresponding angle.

a consequence, we can derive a spectrum without noise of stray light lines (Fig. 4) by integration along the slit of an image taken high in the corona (at about 800 arcsec above the limb). From Fig. 4 we can extract profiles and ratios of the intensities of stray light lines with respect to the C II lines which are chromospheric lines, and above the limb we observe only scattered light. Assuming that the ratios of intensities of lines due to scattered light do not change with the distance to the solar limb, we can also calculate the intensity ratio of scattered lines with respect to the C II 103.6 nm line: H I *Ly* β/C II, O VI 103.2/C II, O VI 103.7/C II. These quantities give us the amount of scattered light in a given line in connection with the intensity of the C II lines. We adopt the same hypothesis for the profiles of scattered lines.

Considering the above hypothesis and using the spectrum of scattered light (and the ratios of the intensities of the scattered lines), we can now build images of scattered light corresponding to the observed images. For a given observed image, which is a grid of $512 * 360$ pixels^2, and for each row (which is a spectrum) we can create a corresponding spectrum of scattered light. For each pixel $i (i = 0, 511)$ the intensity due to the scattered light alone is given by: $(I_s(i)/I_{s,CII}) * I_{CII}$. Where:

- I_{CII}: is the intensity of the C II line in a row of the observed image.
- $I_{s,CII}$: is the intensity of the C II line in the spectrum of scattered light.
- $I_s(i)$: is the intensity of the scattered light in the pixel i in the spectrum of scattered light and provides the profile of lines of scattered lines.

We suppose that the scattered light line shift does not vary with the distance to the solar limb. Consequently, to obtain the spectral positions of the scattered lines, we refer to the positions of the C II lines.

5. Building of the raster images

After reducing the data by correction of the instrumental imperfections (nonuniform sensitivity and geometric distortion of the detector and scattering of light by the telescope mirror), information about the polarization of the O VI 103.2 nm line can be derived. The first task to perform is the building of the monochromatic images for each raster sequence (each angle of rotation). The monochromatic image of a given line is built by integration over the full profile for each slit position in the raster. The slit width of 4 arcsec moved every telescope's steps (3.8 arcsec) provides a good sampling of the solar coronal image. The images provided by the rasters have a width of 120 arcsec at 0° and 60 arcsec for the other angles.

The monochromatic images have been built for each raster sequence and for each line (O VI 103.2 nm line and O VI 103.7 nm line). The superposition of the monochromatic images with respect to their angles of observation (angle made between

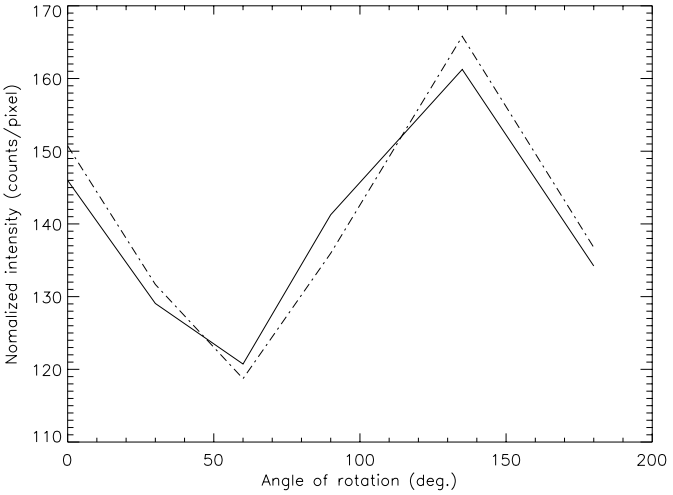

Fig. 6. The variations of the normalized intensities integrated over the common area of the monochromatic images in the two lines 103.2 nm and 103.7 nm of the O VI ion are plotted as a function of the angular position of the slit. The solid line shows the variation of the intensity of the O VI 103.2 nm line and the dashed line shows that of O VI 103.7 nm line multiplied by 2.9. These variations are approximately the same and are probably caused by the solar variations during the time of observation. These solar variations are essentially caused by the polar plumes crossing the field of view. The effect of the O VI 103.2 nm line polarization is weak and masked by the solar variations.

the slit and the north-south polar axis of the sun), is shown on Fig. 5; images built by the different raster have a common area. This common portion corresponds to the same area in the solar corona, seen at different angles by the spectrometer (analyser of polarization), thus the O VI 103.2 nm line (polarization sensitive) and the O VI 103.7 nm line (polarization unsensitive) are observed at the same time under different angles.

At the beginning or at the end of several rasters, the spacecraft was still rolling by few degrees. The data taken during these phases have been rejected and the corresponding raster width are smaller (e.g. $60°$, $90°$, and $180°$) in Fig. 5.

6. Results and discussion

In Fig. 6 the variations of the integrated intensities of O VI 103.2 nm and O VI 103.7 nm lines over the common area are plotted as a function of the orientation of the instrument in respect with the projected polar axis of the sun. The large variation observed is similar for the two O VI lines: the O VI 103.2 nm partially and linearly polarized line and the O VI 103.7 nm unpolarized line. So the main contribution is due to local solar variation, to a great extent probably due to polar plumes crossing the field of view during the fourteen-hour observations.

To eliminate this time dependent intensity variation we exploit the different properties of the two O VI lines. The O VI 103.7 nm is not sensitive to polarization and can be used as a reference for time dependent intensity variation. So the ratio of the intensities of the two lines of the O VI ion ($I_{O_{VI}103.2}/I_{O_{VI}103.7}$) does not depend on time. It changes only with the distance to the solar limb. This ratio is not sensitive to the solar variations and its variation with the angle of observation gives only the effect of the polarization of the O VI 103.2 nm line. In our case we will neglect the variation of the ratio $I_{O_{VI}103.2}/I_{O_{VI}103.7}$ with the distance to the solar limb, because we integrate the intensities over the same small area and we suppose that this variation is also too small to be taken into consideration.

The ratio of the intensities of the two lines of the O VI ion ($I_{O_{VI}103.2}/I_{O_{VI}103.7}$) is found to be close to 2.9. This ratio is greater than 2 (the expected value for only collisional excitation), so there is a strong contribution of photoexcitation (condition required for resonance fluorescence scattering and polarization). The variation of this ratio with the angle of observation is shown by Fig. 7. The fit of the variation of the ratio ($I_{O_{VI}103.2}/I_{O_{VI}103.7}$) with a sinusoidal function gives a period equal to $180°$ (solid line in the same figure). It presents a maximum at less than $90°$ and a minimum at less than $180°$. The degree of correlation between the variation of the ratio of the intensities of the O VI lines and the sinusoidal fit is equal to 0.93. The error bars are determined from only statistical considerations based on the number of counts for each line. The statistical errors which may be introduced by the correction of the scattered light and the flat field were also taken into account.

From the previous remarks we can infer that the variation with the angle of observation of the $I_{O_{VI}103.2}/I_{O_{VI}103.7}$ ratio is due to the linear polarization of the O VI 103.2 nm partially polarized line. The rate of modulation of the ratio $I_{O_{VI}103.2}/I_{O_{VI}103.7}$ with the angle of observation is found almost equal to 3.8%. Such a rate of modulation is related to the linear polarization of the O VI 103.2 nm line through the analyse of polarization performed by the instrument.

7. Conclusion

As it has been mentioned in the introduction, the aims of this paper are the detection and the study of the polarization of the O VI 103.2 nm line using the SUMER's observations.

Using SUMER-SOHO observations in the coronal south polar hole of the Sun and exploiting the sensitivity of SUMER to the polarization of an incident linear polarized light, we have detected a modulation of the O VI 103.2 nm line intensity with angle of rotation of the spacecraft. The detected signal shows a sinusoidal fluctuation of the ratio $I_{O_{VI}103.2}/I_{O_{VI}103.7}$ We have determined the amplitude of the modulation (3.8%) which is related to the analyse of linear polarization.

This work will be continued in order to determine the three Stokes parameters of the O VI 103.2 nm line (direction and linear polarization). Then the results will be used to study the Hanle and dimming effects affecting this transition, with the purpose of obtaining information on the magnetic field and velocity field vectors.

Acknowledgements. We thank K. Wilhelm for discussion which helps to perform the observations, and I. Buettner and N. Morisset who operate the SUMER spectrometer during the observations. The SUMER project is financially supported by DLR, CNES, NASA, and ESA PRODEX programme (Swiss contribution). The SOHO is a mission of international cooperation between ESA and NASA.

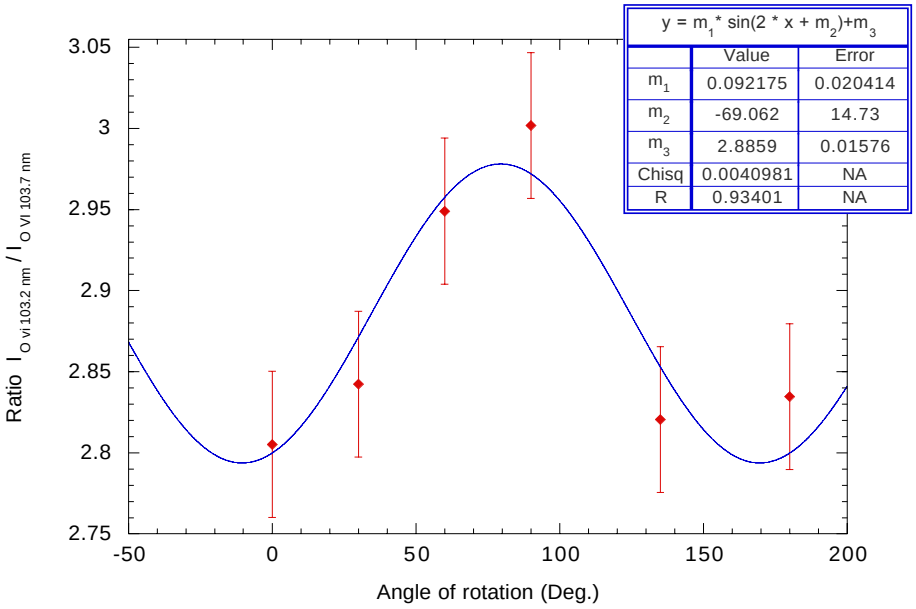

Fig. 7. The variation of the ratio of the intensities of two resonance lines of the O VI ion integrated over the common area is plotted as a function of the angular orientation of the instrument (diamonds). The mean value of this ratio is ≈ 2.9. A sinusoidal function (solid line) fits well the variation (within the error bars). This variation reflects only the effect of the O VI 103.2 nm line polarization since that the ratio of the intensities of two lines of the O VI ion is independent of the solar variation. The error bars are determined only by statistical considerations based on photon counting statistics (taking into account errors due to the different corrections).

References

Beckers J.M., Chipman E., 1974, Solar Phys. 34, 151

Bommier V., Sahal-Bréchot S., 1978, A&A 69, 57–64

Bommier V., Leroy J.L., Sahal-Bréchot S., 1986, A&A 156, 79–89

Bommier V., Landi Degl'Innocenti E., Leroy J.L., Sahal-Bréchot S., 1994, Solar Phys. 154, 231

Brekke P., Hassler D.M., Wilhelm K., 1997, Solar Phys. 175, 349–374

Doschek G.A., Warren H.P., Laming J.M., et al., 1997, ApJ 482, L109–L112

Gabriel A.H., 1971, Solar Phys. 21, 392

Hassler D.M., Wilhelm K., Lemaire P., Schühle U., 1997, Solar Phys. 175, 375–391

Hassler D.M., Lemaire P., Longval Y., 1997, Applied Optics 36, 353–359

Judge P., Carlsson M., Wilhelm K., 1997, ApJ 490, L195–L198

Kohl J.L., Withbroe G.L., 1982, ApJ 256, 263

Kohl J.L., Noci G., Antonucci E., et al., 1998, ApJ 501, L127–L131

Lemaire P.,Wilhelm K., Curdt W., et al., 1997, Solar Phys. 170, 105–122

Li X., Shadia Rifai Habbal, Kohl J.L., Noci G., 1998, ApJ 501, L133–L137

Moran T., 1996, http://sohoww.nascom.nasa.gov/solarsoft/sohosumer/idl/contrid/moran

Reeves E.M., Parkinson W.H., 1970, ApJS 181, vol. 21, An Atlas of Extreme-Ultraviolet Spectroheligrams from OSO-IV

Sahal-Bréchot S., 1974, A&A 36, 147–154, paper I

Sahal-Bréchot S., 1974, A&A 36, 355–363, paper II

Sahal-Bréchot S., 1977, ApJ 213, 887–899

Sahal-Bréchot S., 1981, Space Sci. Rev. 29, 391–401

Sahal-Bréchot S., Bommier V., Leroy J.L., 1977, A&A 59, 223–231

Sahal-Bréchot S., Bommier V., Feautrier N., 1998, A&A 340, 579

Sahal-Bréchot S., Malinovsky M., Bommier V., 1986, A&A 168, 284–300

Sahal-Bréchot S., Feautrier N., Bommier V., de Kertanguy A., In: Damé L., Guyenne T.D. (eds.) Stokes parameters of the O VI 103.2 nm line as a probe of the matter velocity field in the solar wind acceleration region. ESA workshop on solar physics and astrophysics at interferometric resolution, Paris 17–19 February 1992, ESA special publication SP-344, pp. 81–85

Vial J.-C., Lemaire P., Artzner G., Gouttebroze P., 1980, Solar Phys. 68, 187–206

Wilhelm K., Curdt W., Marsch E., et al., 1995, Solar Phys. 162, 189–231

Wilhelm K., Lemaire P., Curdt W., et al., 1997, Solar Phys. 170, 75–104

Withbroe G.L., Kohl J.L., Weiser H., Noci G., Munro R.H., 1982a, ApJ 254, 361

Withbroe G.L., Kohl J.L., Weiser H., Munro R.H., 1982b, Space Sci. Rev. 33, 17